

A Refraction Seismic Image of the Sediments in Kennedy Channel, Northern Nares Strait

by Thomas Funck^{1*}, Sonya A. Dehler², H. Ruth Jackson², Matthew H. Salisbury² and Ian D. Reid³

Abstract: A refraction / wide-angle reflection seismic study was carried out in the 35-km wide Kennedy Channel in northern Nares Strait between Greenland and Ellesmere Island, Canada. The objective was to study the uppermost subsurface structure in the channel, where a hypothesized strike-slip fault (Wegener Fault) could mark the plate boundary between Greenland and North America. Three land-stations (one on either side of the channel and a third one on Hans Island) recorded densely spaced airgun shots along three lines. However, ice conditions limited the observations in the western part of the channel. With the given shot–receiver offsets of <44 km, the velocity structure of the uppermost sediment layer could be determined by forward and inverse modeling. This layer has P-wave velocities of 5.8 to 5.9 km s⁻¹ in the west and 6.1 to 6.2 km s⁻¹ in the east. The Poisson's ratios vary between 0.28 and 0.31 in the west, and between 0.31 and 0.32 in the east. The lateral velocity change occurs close to Hans Island. From the obtained velocities it is inferred that the sediment layer consists of carbonates. P-wave velocity measurements on a limestone sample from Greenland (5.9 to 6.1 km s⁻¹) are compatible with the high velocities found in the channel. In eastern Kennedy Channel, the base of the carbonate layer shallows towards the north, from 4.5 km to 3.5 km over a lateral distance of c. 10 km. West of Hans Island, the base of the carbonate layer is not constrained. Absence of sharp offsets at the base of the carbonates make it not very probable that a major strike-slip fault runs through the eastern part of Kennedy Channel. This is consistent with observations from bathymetric and reflection seismic data, which show a steep fault just west of Hans Island.

Zusammenfassung: Eine Refraktions- und Weitwinkel-reflexionsseismische Vermessung wurde im 35 km breiten Kennedy Channel in der nördlichen Nares Strait zwischen Grönland und Ellesmere Island (Kanada) durchgeführt. Das Ziel war es, die oberste Untergrundstruktur des Kanals zu untersuchen, wo eine hypothetische Blattverschiebung (Wegener-Verwerfung) die Plattengrenze zwischen Grönland und Nordamerika anzeigen könnte. Drei Landstationen (eine auf jeder Seite des Kanals und eine dritte auf Hans Island) registrierten kurzabständige Schüsse von Luftkanonen. Aufgrund der Eisbedingungen waren Beobachtungen im westlichen Teil des Kanals jedoch nur eingeschränkt möglich. Mit den gegebenen Abständen Schuss–Rekorder von weniger als 44 km konnte die Geschwindigkeitsstruktur in der obersten Sedimentschicht durch Vorwärtsmodellierung und Inversion ermittelt werden. Diese Schicht hat P-Wellengeschwindigkeiten von 5.8–5.9 km s⁻¹ im Westen und 6.1–6.2 km s⁻¹ im Osten. Im Westen variiert die Poissonzahl zwischen 0.28 und 0.31, im Osten zwischen 0.31 und 0.32. Die laterale Geschwindigkeitsänderung tritt in der Nähe von Hans Island auf. Aus den ermittelten Geschwindigkeiten lässt sich ableiten, dass die Sedimentschicht aus Karbonaten besteht. Messungen der P-Wellengeschwindigkeit an einer Kalksteinprobe von Grönland (5.9–6.1 km s⁻¹) stehen im Einklang mit den im Kanal ermittelten hohen Geschwindigkeiten. Die Basis der Karbonatschicht im östlichen Kennedy Channel wird zum Norden hin flacher, von 4.5 auf 3.5 km über einen Abstand von ca. 10 km. Westlich von Hans Island ist die Basis der Karbonatschicht praktisch nicht erfasst. Das Fehlen von abrupten Verwerfungen an der Basis der Karbonate lässt es nicht wahrscheinlich erscheinen, dass eine größere Blattverschiebung durch den östlichen Kennedy Channel verläuft. Dies steht im Einklang mit Beobachtungen aus bathymetrischen und reflexionsseismischen Daten, welche eine steil einfallende Verwerfung dicht westlich von Hans Island zeigen.

INTRODUCTION

The Nares Strait controversy as discussed in DAWES & KERR (1982a) is about whether or not the strait is the plate boundary between Greenland and North America, and, if so, how much strike-slip movement occurred along this boundary. DAWES & KERR (1982b) argue that there is little or no strike-slip displacement along Nares Strait, on the basis of present-day continuity of geological features from Ellesmere Island, Canada, to Greenland. However, based on plate tectonic reconstructions, SRIVASTAVA (1985) suggests that Greenland moved 150 km northwards relative to North America, most of which should have been taken up by sinistral strike-slip movement in Nares Strait. Hence, there is an apparent incompatibility between the onshore geology surrounding Nares Strait and plate tectonic models describing the opening of the North Atlantic and the resulting motions of Greenland.

It is clear that the controversy can only be resolved by detailed mapping of the strait itself to find indications for one model or the other. Therefore, a multidisciplinary experiment was carried out in August–September 2001, including geological field work onshore and regional geophysical measurements to extend the interpretations offshore. In northern Nares Strait, a refraction seismic transect was carried out across Kennedy Channel (Fig. 1). The main objective of the transect was to obtain velocity information from the sediments to improve the processing and interpretation of the reflection seismic data, and the transect length of just 46 km is too short to provide information about the deeper crustal velocity structure. However, we have also analyzed the refraction seismic data in terms of what they can contribute to the Nares Strait debate.

GEOLOGICAL SETTING

The study area (Fig. 1) in Kennedy Channel in northern Nares Strait is part of the lower Palaeozoic Franklinian Basin. The basin sequence is intensely folded in the Late Devonian to Early Carboniferous Ellesmerian Fold-and-Thrust belt on Ellesmere Island (MAYR et al. in press), while it is undeformed on the Ellesmerian foreland of Greenland. Onshore Greenland, in Washington Land, the coastal outcrops belong to the Middle Ordovician to Lower Silurian Morris Bugt Group, to the Lower to Upper Silurian Peary Land Group, and in the north to the Lower Silurian Washington Land Group (DAWES 2000). The exposed units on Hans Island, in the middle of Kennedy Channel, belong to the Washington Land group and consist of near-horizontal platform carbonates. Onshore Ellesmere Island, carbonates and siliciclastic rocks predominate (MAYR et al. in press).

¹ Danish Lithosphere Centre, Øster Voldgade 10 L, 1350 Copenhagen K, Denmark; * now at: Geological Survey of Denmark and Greenland, Øster Voldgade 10, 1350 Copenhagen K, Denmark.

² Geological Survey of Canada (Atlantic), Bedford Institute of Oceanography, P.O. Box 1006, Dartmouth, Nova Scotia, B2Y 4A2, Canada.

³ Geological Institute, University of Copenhagen, Øster Voldgade 10, 1350 Copenhagen K, Denmark.

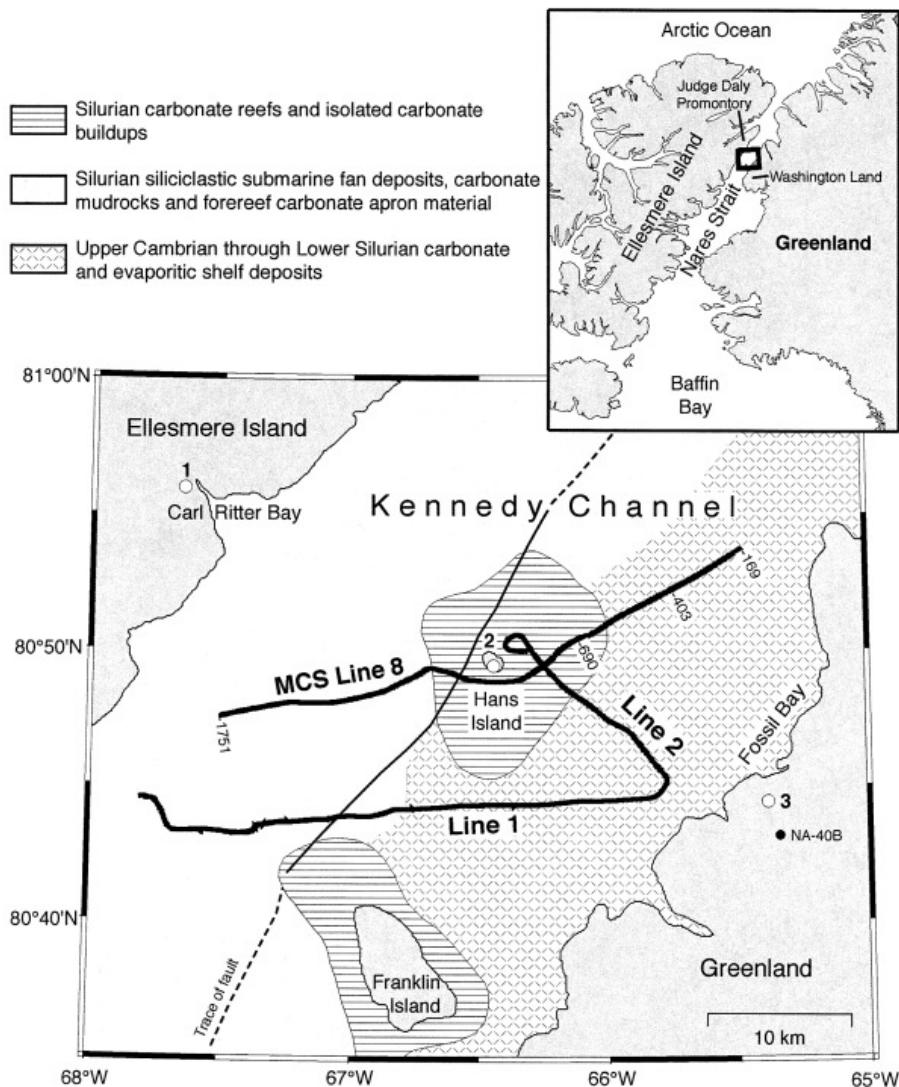


Fig. 1: Regional geology map of Kennedy Channel (HARRISON, in press). Bold lines show the location of the segments with airgun shots. Labels along MCS line 8 indicate shot point numbers. Seismic recorders are indicated by open circles and annotations specify the station number. The solid and dashed line in the middle of Kennedy Channel show the steep fault mapped by Jackson et al. (2006). The filled circle shows the location of limestone sample NA-40B from Fossil Bay.

Harrison (in press) distinguishes between two major geological units within Kennedy Channel (Fig. 1). In the western part, the seafloor is characterized by Silurian siliciclastic submarine fan deposits, carbonate mudrocks and fore-reef carbonate apron material. In the east, Upper Cambrian through Lower Silurian carbonate and evaporitic shelf deposits are encountered. Around Hans Island, carbonate reefs and isolated carbonate buildups are mapped, which correlate with similar deposits in Washington Land and adjacent islands of northern Nares Strait.

Based on bathymetric data and on reflection seismic records, JACKSON et al. (2006) trace a major fault through Kennedy Channel (Fig. 1). New mapping on Ellesmere Island (MAYR et al. in press) has revealed a network of strike-slip faults in coastal areas of northeastern Ellesmere Island, which is best exposed on Judge Daly Promontory. This suggests that part of the Wegener Fault – the large hypothetical transform fault between Greenland and Canada – is exposed onshore on Ellesmere Island. The Wegener Fault is an important element of plate reconstructions in which Greenland moved northward relative to Ellesmere Island in the Late Cretaceous and Tertiary (e.g., SRIVASTAVA 1985).

WIDE-ANGLE SEISMIC EXPERIMENT

Data acquisition

The refraction seismic survey (Fig. 1) in Kennedy Channel was carried out 20 to 21 August 2001 onboard the Canadian Coast Guard ship CCGS “Louis S. St.-Laurent”. The original intent of the experiment (Fig. 1) was to have a straight line across Kennedy Channel connecting the seismic recorders in Carl Ritter Bay on Ellesmere Island (station 1), on Hans Island (station 2) and in Fossil Bay in Greenland (station 3). However, high winds during the deployment of the three ORION land stations (equipped with three-component geophones) pushed the ice towards the Ellesmere Island coast and prevented shooting in the vicinity of Carl Ritter Bay. The modified shooting program consisted of an E–W line running from Ellesmere Island towards the station in Fossil Bay (line 1), and an adjoining line between Fossil Bay and Hans Island (line 2).

The seismic source for lines 1 and 2 was an airgun array consisting of six Sodera GI-guns with a total volume of 1230 cubic inches (20.2 L) fired every 15 seconds. This provided an average shot spacing of 28 m on line 1 and 36 m on line 2. Timing and positioning of shots and seismic recorders were

determined by the Global Positioning System (GPS).

During the deployment of the land stations, CCGS “Louis S. St-Laurent” ran multi-channel seismic (MCS) line 8 (Fig. 1) close to Hans Island. Part of this line was recorded by the ORION receivers. Station 1 recorded shots 403 through 1751, station 2 shots 169 through 1751, and station 3 shots 690 through 1751. For MCS line 8, only three of the Soderia GIGs with a total volume of 615 cubic inches (10.1 L) were used. Shot spacing was 25 m and shot times were recorded by the internal clock of the MCS acquisition unit. This internal clock was later calibrated to GPS time by using the seismic records at the cross point of line 2 and MCS line 8.

Data processing

After retrieval of the land recorders, the seismic data were dumped, converted to SEG-Y format and subsequently debiased. Deconvolution was applied to sharpen the wavelet. All record sections shown in Figures 2 through 5 are band-pass filtered from 4 to 10 Hz and are displayed with a reduction velocity of 7.0 km s⁻¹. Traces are weighted by their distance to the station to increase the amplitudes for large offsets.

Methodology

The greatest challenge for the velocity modeling was that the experiment was not two-dimensional, particularly for lines 1 and 8. However, the distribution of shot observations and receivers was not sufficient to warrant a proper three-dimensional modeling approach in the form of a regional tomographic study. As it turned out, the final velocity models suggest that two-dimensional modeling is adequate in this case.

The velocity models for the three lines were developed using the program RAYINVR (ZELT & SMITH 1992, ZELT & FORSYTH 1994). The uppermost layer in the model is the water layer and the water depth was obtained from the ship’s echosounder. Water depths on lines 1 and 2 are shown with respect to their distance from station 3. On line 8, water depths are shown with respect to their distance from station 2. To take account of the fact that the receivers were located on land and not in the water, static corrections were applied. The data were insufficient to resolve more than a single layer. *P*-wave velocities within this layer and the depth to the base of the layer were first determined by forward modeling, and later optimized by inverse modeling. Different phase velocities in the western and eastern part of the channel were easily recognizable from the record sections. The modeling strategy was to use the inver-

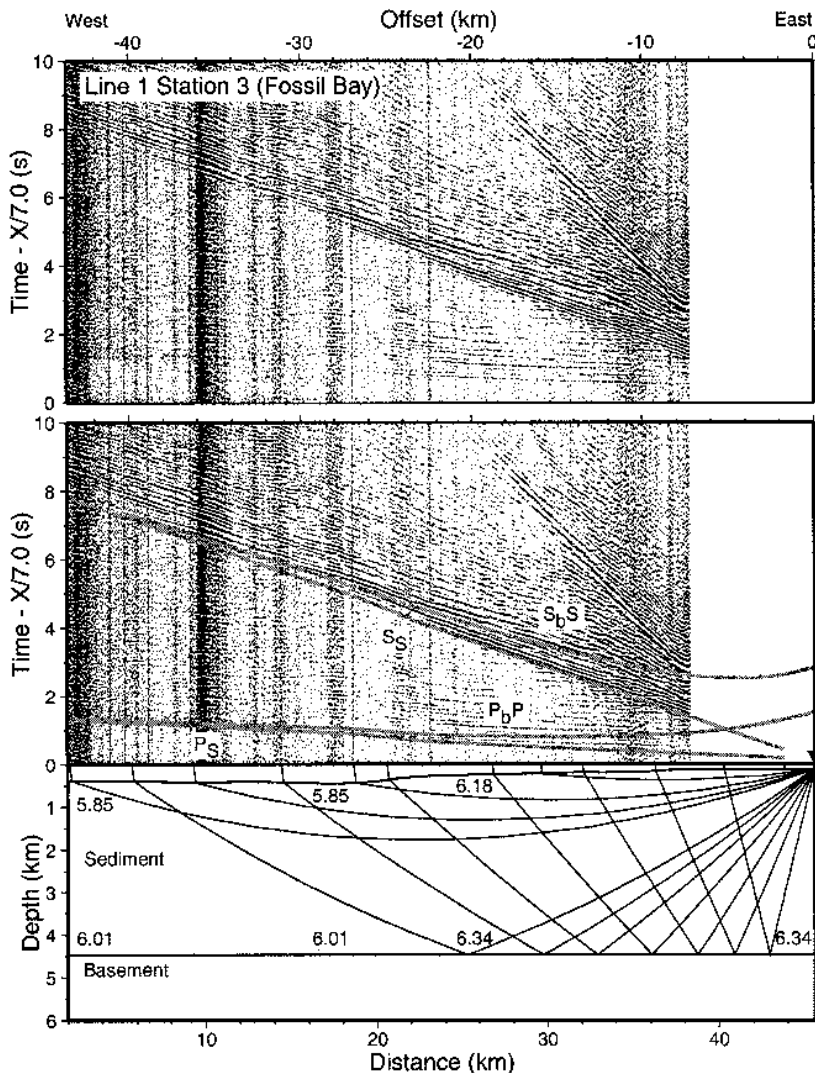


Fig. 2: Record section with (middle) and without (top) computed travel times and ray path diagram (bottom) for the vertical geophone component of station 3 (Fossil Bay, Greenland) for line 1. Horizontal scale in the record section is shot-receiver distance (offset) and the vertical scale is the travel time using a reduction velocity of 7.0 km s⁻¹. A triangle indicates the receiver location. See text for the description of phases. Processing includes deconvolution and a band-pass filter from 4 to 10 Hz. Traces are weighted by their distance to the station. The horizontal scale in the ray path diagram is distance along the velocity model (Fig. 7). Numbers in the model (bottom) indicate computed *P*-wave velocity in km s⁻¹.

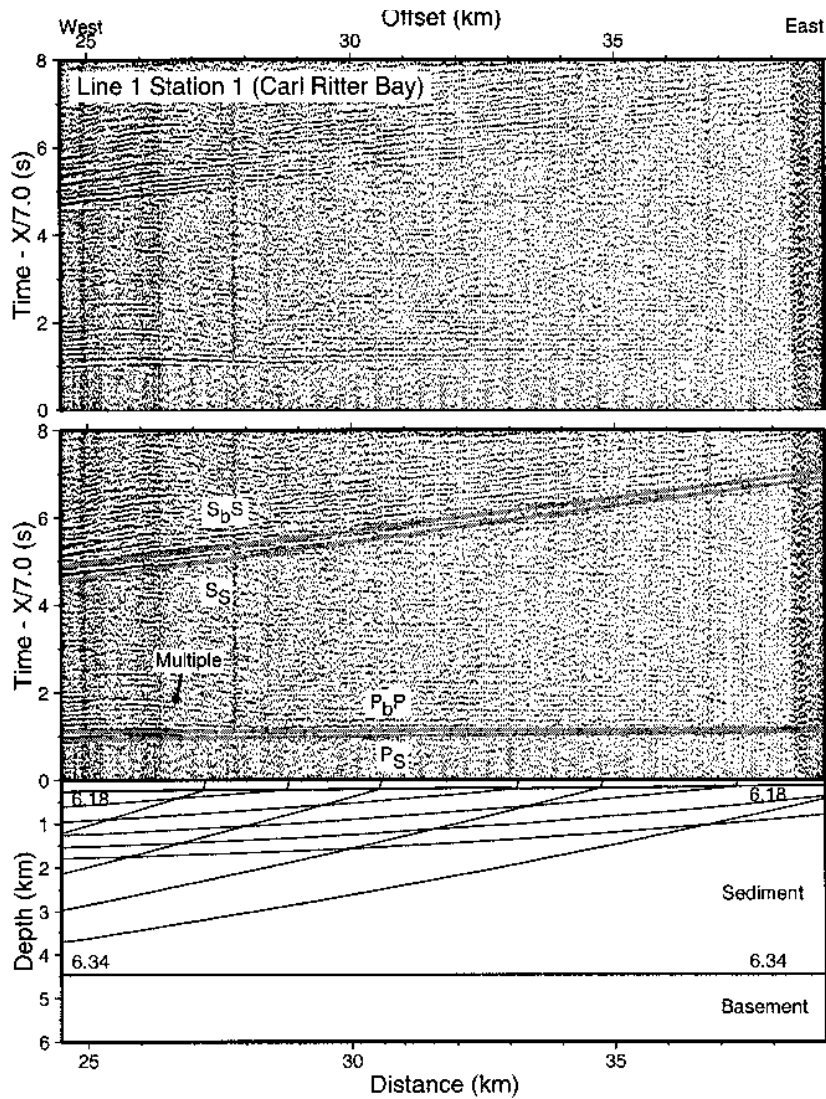


Fig. 3: Record section with (middle) and without (top) computed travel times (top) and ray path diagram (bottom) for the vertical geophone component of station 1 (Carl Ritter Bay, Ellesmere Island) for line 1. Horizontal scale in the record section is shot-receiver distance (offset) and the vertical scale is the travel time using a reduction velocity of 7.0 km s^{-1} . See text for the description of phases. Processing includes deconvolution and a band-pass filter from 4 to 10 Hz. Traces are weighted by their distance to the station. The horizontal scale in the ray path diagram is distance along the velocity model (Fig. 7). Numbers in the model (bottom) indicate computed P -wave velocity in km s^{-1} .

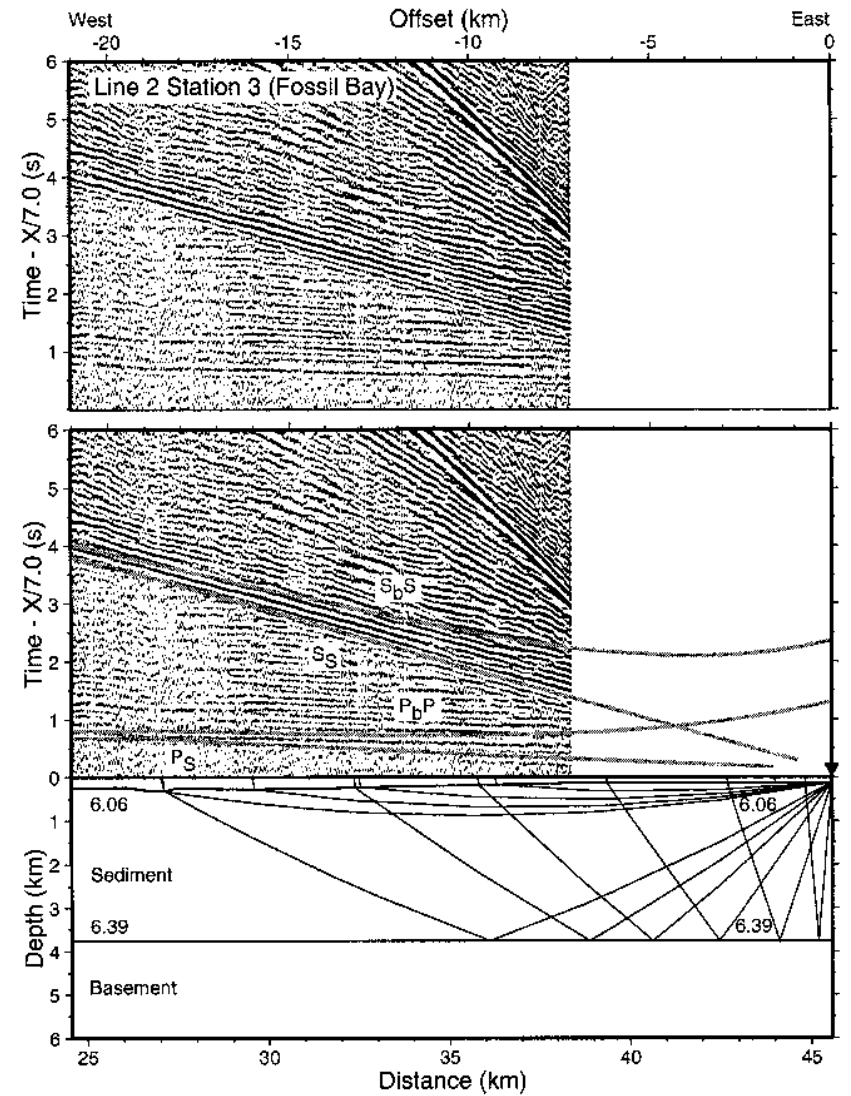


Fig. 4: Record section with (middle) and without (top) computed travel times (top) and ray path diagram (bottom) for the vertical geophone component of station 3 (Fossil Bay, Greenland) for line 2. Horizontal scale in the record section is shot-receiver distance (offset) and the vertical scale is the travel time using a reduction velocity of 7.0 km s^{-1} . A triangle indicates the receiver location. See text for the description of phases. Processing includes deconvolution and a band-pass filter from 4 to 10 Hz. Traces are weighted by their distance to the station. The horizontal scale in the ray path diagram is distance along the velocity model (Fig. 7). Numbers in the model (bottom) indicate computed P -wave velocity in km s^{-1} .

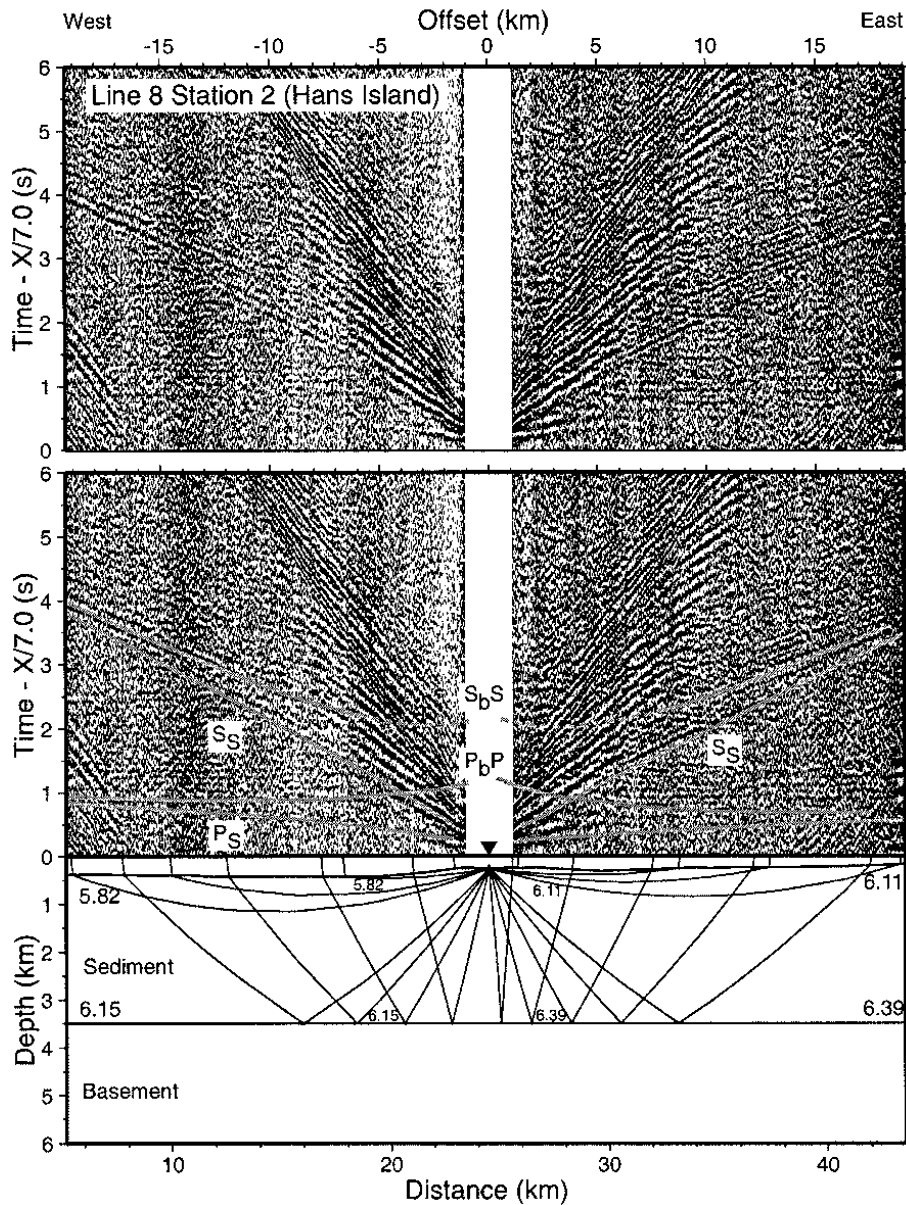


Fig. 5: Record section with (middle) and without (top) computed travel times (top) and ray path diagram (bottom) for the vertical geophone component of station 2 (Hans Island) for MCS line 8. Horizontal scale in the record section is shot-receiver distance (offset) and the vertical scale is the travel time using a reduction velocity of 7.0 km s^{-1} . A triangle indicates the receiver location. See text for the description of phases. Processing includes deconvolution and a band-pass filter from 4 to 10 Hz. Traces are weighted by their distance to the station. The horizontal scale in the ray path diagram is distance along the velocity model (Fig. 7). Numbers in the model (bottom) indicate computed P-wave velocity in km s^{-1} .

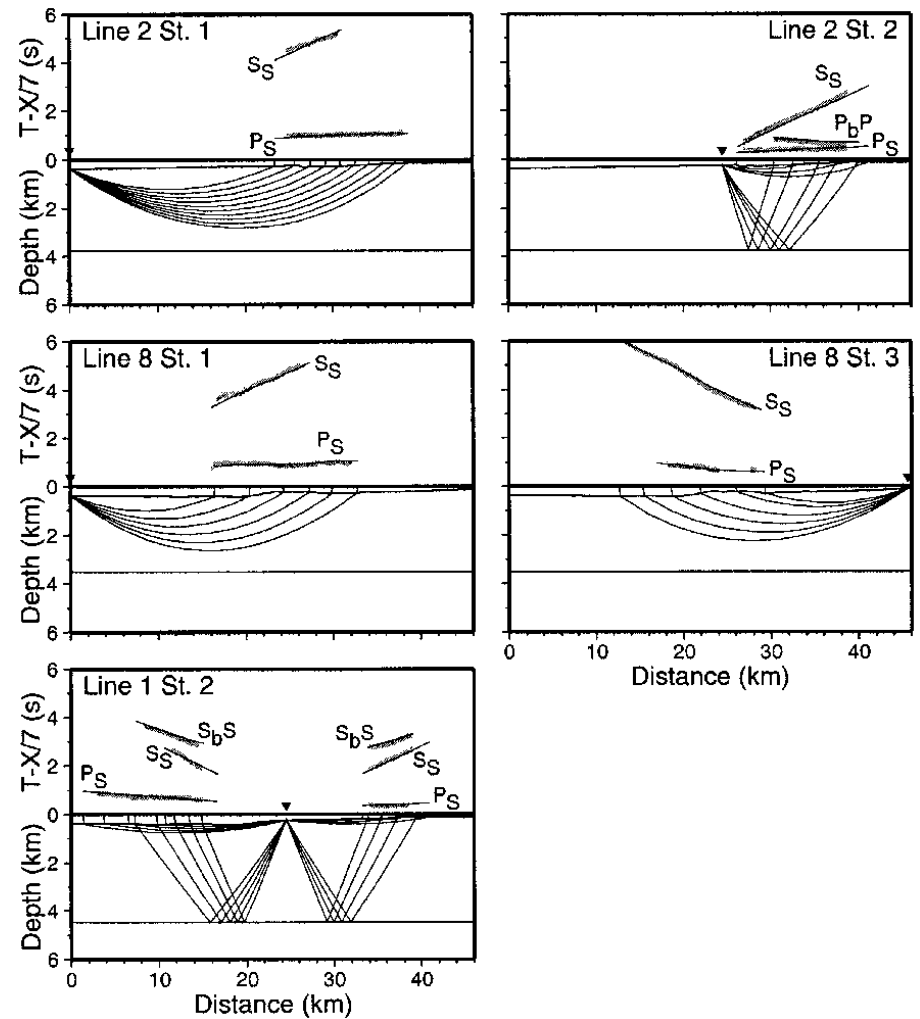


Fig. 6: Comparison of observed and calculated travel times (for record sections not shown in Figs. 2 through 5), shown together with the corresponding ray paths. Note that the ray paths are shown for the P phases. Observed data are indicated by vertical grey bars with heights representing pick uncertainty; calculated data are indicated by solid lines. Triangles mark the receiver locations. Horizontal scale is the model position; a reduction velocity of 7.0 km s^{-1} has been applied for the travel times.

sion algorithm to find the optimum value for the velocity in the western and eastern blocks of the model. No lateral variations were allowed within each of the blocks. After the velocities were determined, the location of the transition zone between the two blocks was optimized. Finally, S -wave velocity models were developed and Poisson's ratios were calculated from the observed P and S -wave velocities.

Seismic data

The data quality is generally good as can be seen on the record sections in Figures 2 through 5. The signal-to-noise ratio for MCS Line 8 (Fig. 5) is lower than for lines 1 and 2 because of the smaller volume of the airgun array.

Given that maximum shot-receiver offset was 44 km, only phases from the uppermost sediment layer are observed. Both P - and S -wave refractions (P_s and S_s , respectively) from this layer can be seen (Figs. 2 through 5). Typical phase velocities of the P_s and S_s phase are 6.0-6.2 km s⁻¹ and 3.0-3.2 km s⁻¹, respectively. P -wave and S -wave reflections from the base of the sediment layer are labeled P_bP and S_bS , respectively. In general, the S_bS phase is more prominent than the P_bP phase. This is due to the greater delay of the shear wave reflection with respect to the S_s refraction, giving less interference between these two phases than is the case for the P -wave field.

Some multiples of the primary refractions almost look like reflections. For example, on the record of line 1 at Carl Ritter Bay (station 1) there is a pronounced bend in the multiple at an offset of 26.5 km (Fig. 3), which could be easily misinterpreted as the P_bP reflection. The bend in the multiple is related to the rather sudden eastward shallowing of the water close to the middle of Kennedy Channel.

RESULTS

Velocity models

The raytracing through the velocity models is shown in Figures 2 through 6, while the final velocity models are displayed in Figure 7. The sediment layer on line 1 is characterized by a lateral change of the P -wave velocity from 5.85 km s⁻¹ in the west to 6.18 km s⁻¹ in the east, with the change occurring in the middle of Kennedy Channel. The Poisson's ratio σ also changes from 0.30 in the west to 0.32 in the east, based on the P -wave velocities given above and S -wave velocities of 3.13 km s⁻¹ in the west and 3.19 km s⁻¹ in the east. Hence, there is only a slight lateral change in the S -wave velocity (0.06 km s⁻¹) compared to a variation of 0.33 km s⁻¹ in the P -wave velocity. The base of the sediment layer is at a depth of 4.5 km.

Line 2 (Fig. 7) has similar overall features as line 1. P -wave velocity increases from 5.88 km s⁻¹ in the west to 6.06 km s⁻¹ in the east, with the Poisson's ratio increasing from 0.28 to 0.31, since S -wave velocities of 3.25 km s⁻¹ and 3.17 km s⁻¹ are observed in the west and east, respectively. The velocity change occurs over a narrow transition zone close to Hans Island. Velocities are overall very similar to line 1. However, the base of the sediment layer at a depth of 3.75 km is shallower than on line 1.

The velocity model for MCS line 8 (Fig. 7) shows P -wave velocities of 5.82 km s⁻¹ and 6.11 km s⁻¹ to the west and east of Hans Island, respectively. S -wave velocities are 3.05 km s⁻¹ (Poisson's ratio $\sigma = 0.31$) in the west and 3.15 km s⁻¹ ($\sigma = 0.32$) in the east. The base of the sediments is at a depth of 3.5 km.

Error analysis

Travel time residuals, the number of observations, and normalized χ^2 for individual phases and lines are summarized in Tables 1 through 3. Note that only travel time picks of every fourth trace were used for the modeling due to the dense shooting. The total root-mean-square (rms) misfit varies between 56 and 64 ms on individual lines, which translates into a normalized χ^2 between 0.318 and 0.432 for the assumed pick uncertainty of 100 ms. A χ^2 of 1.0 is the optimum value, with values <1.0 indicating that the model is fitted to the noise in the data. However, the pick uncertainty is a rather subjective parameter and decreasing the uncertainty will increase the χ^2 value. It should also be noted that the uppermost layer in a velocity model is often better constrained than deeper layers, as it is not affected by uncertainties in the overlying layers.

Phase	n	t_{rms} (ms)	χ^2
P_s	440	0.052	0.273
S_s	292	0.043	0.185
P_bP	47	0.034	0.118
S_bS	340	0.090	0.810
All phases	1119	0.064	0.406

Tab. 1: Number of observations (n), RMS misfit between calculated and picked travel times (t_{rms}), and normalized χ^2 for individual phases on Line 1.

Phase	n	t_{rms} (ms)	χ^2
P_s	342	0.026	0.068
S_s	278	0.076	0.584
P_bP	159	0.061	0.370
S_bS	38	0.064	0.425
All phases	817	0.056	0.318

Tab. 2: Number of observations (n), RMS misfit between calculated and picked travel times (t_{rms}), and normalized χ^2 for individual phases on Line 2.

Phase	n	t_{rms} (ms)	χ^2
P_s	266	0.068	0.456
S_s	414	0.071	0.503
P_bP	66	0.035	0.124
S_bS	131	0.057	0.326
All phases	877	0.066	0.432

Tab. 3: Number of observations (n), RMS misfit between calculated and picked travel times (t_{rms}), and normalized χ^2 for individual phases on MCS Line 8.

All three velocity models (Fig. 7) have been kept very simple, each being a minimum-structure model. The base of the sediment layer was kept horizontal. This is certainly a simplification, since out-of line stations were incorporated in the modeling and the three velocity models show a northward thinning of the layer. However, the good fit of the reflectors to the model validates this approach.

To estimate the uncertainty of individual parts of the model, velocity and boundary nodes were varied to see how sensitive the travel times are to changes. Velocities can be changed by

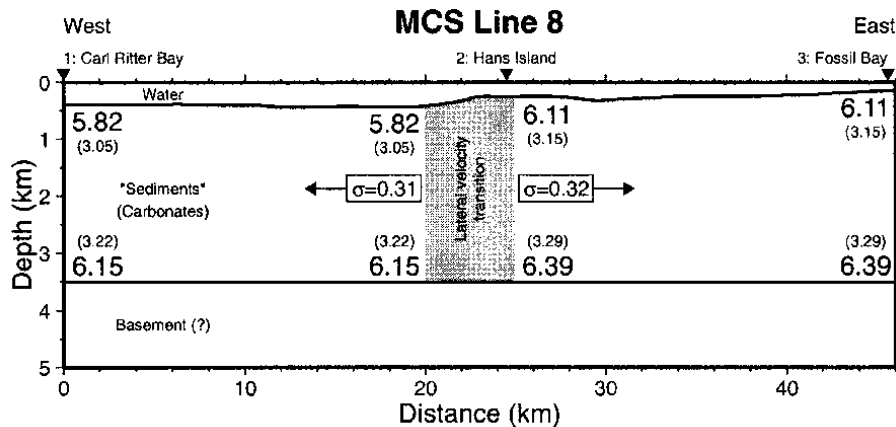
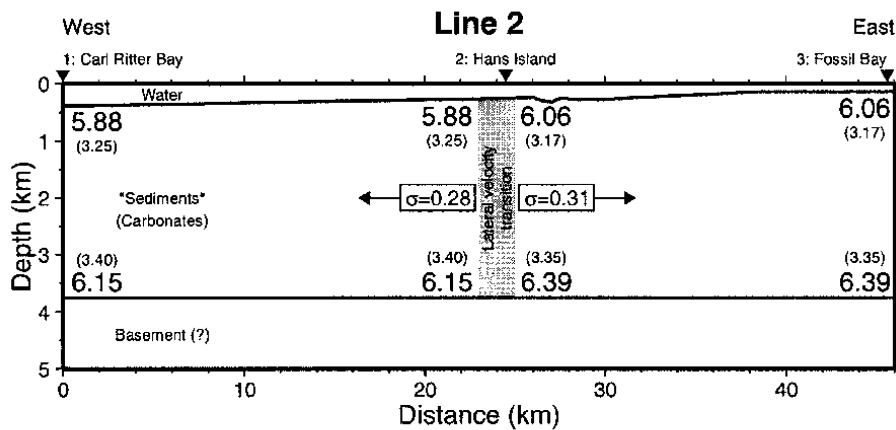
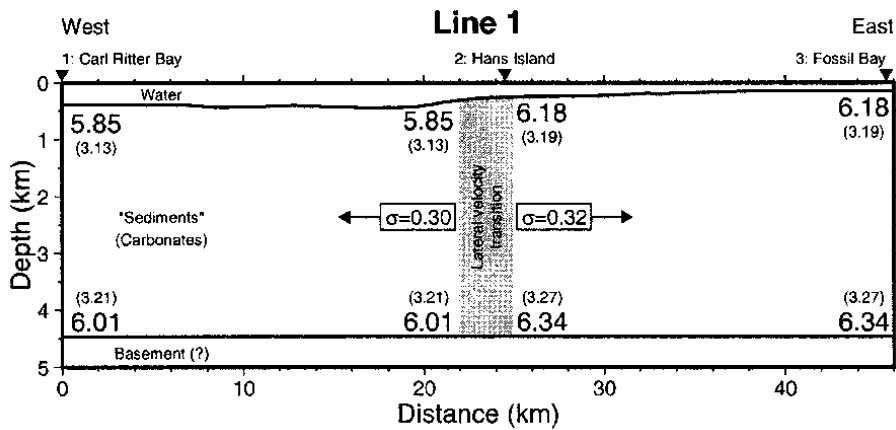


Fig. 7: Velocity models for lines 1 and 2, and for MCS line 8. Large numbers indicate P -wave velocity in km/s; S -wave velocities are shown as small numbers in brackets. The Poisson's ratio (σ) is specified for the western and eastern segment of each line. Grey shading marks the zone where the lateral velocity transition occurs. Triangles indicate the location of receivers.

$\pm 0.1 \text{ km s}^{-1}$ without a major increase of the travel time residuals, while the layer boundary can be moved by $\pm 300 \text{ m}$.

Figure 8 shows the location of the reflection midpoints of all picked P_bP and S_bS arrivals. It is obvious that almost all midpoints lie within the eastern part of Kennedy Channel. Hence, the thickness of the sediment layer in the western part of the channel has to be considered as unconstrained. The only exception is a short reflection branch from line 1 recorded at station 1 (Carl Ritter Bay; Fig. 3). The reflection midpoints of this phase lie 6 km off the coast of Ellesmere Island. However, the observed reflection branch interferes with the P_s arrival and there remains some doubt how well the P_bP is identified on this particular record.

High-pressure velocities of rock sample

To get a sense for the velocities of the carbonates in Kennedy Channel, the velocity of a limestone sample was measured at a high-pressure testing facility operated by the Geological Survey of Canada and Dalhousie University in Halifax, Nova Scotia. The rock sample NA-40B (location $80^\circ 43.13' \text{ N}$, $65^\circ 20.19' \text{ W}$) was from Fossil Bay in Greenland (Fig. 1). Two mini-cores with diameters of 2.54 cm and lengths of c. 3.6 cm were drilled out of this sample, one with the core axis normal to the foliation (sample NA-40B z) and one with the core axis parallel to the foliation (sample NA-40B xy). The P -wave velocities were measured parallel to the core-axis under dry conditions at hydrostatic confining pressures from 10 to 600 MPa using the pulse transmission technique of BIRCH (1960).

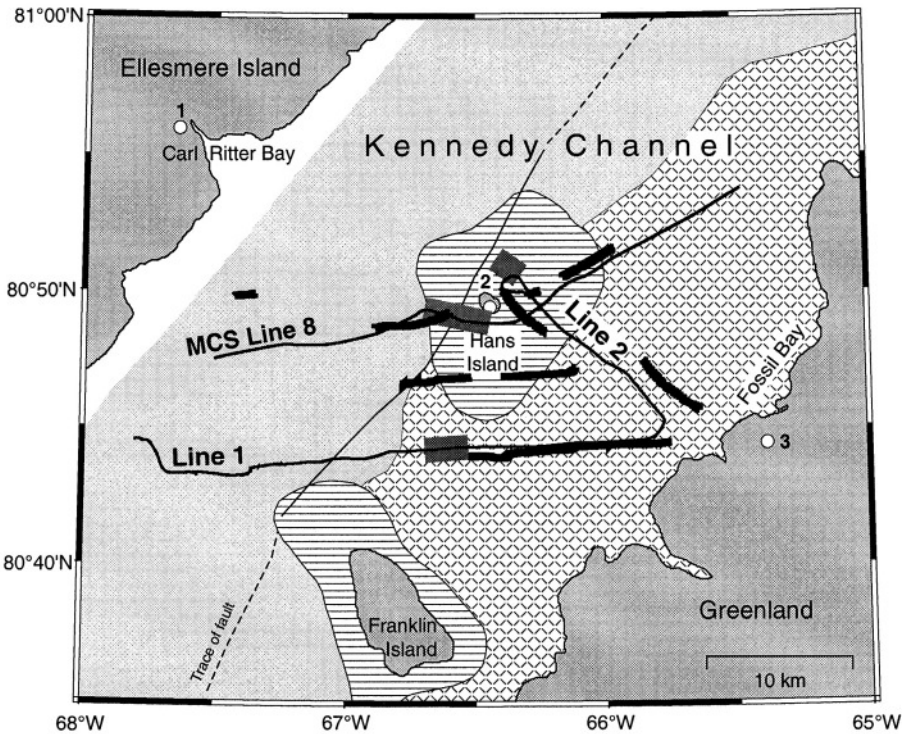
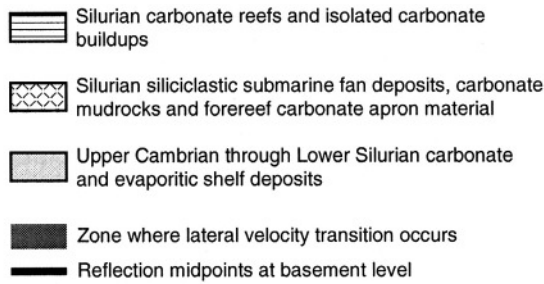


Fig. 8: Geology map of Kennedy Channel (HARRISON in press) (description in Fig. 1). Bold grey lines indicate where the lateral velocity transition occurs along the three refraction seismic lines. Bold black lines show the reflection midpoints of all observed P_rP and S_rS reflections from the base of the carbonates.

Results of the velocity measurements are summarized in Table 4 and in Figure 9. Velocities normal to the foliation are higher than those parallel to the foliation at low pressure. However, the difference between the two mini-cores decreases with increasing pressure. The samples show an initial sharp increase in velocity with increasing pressure but above ca. 200 MPa, the velocity-pressure relationship becomes essentially linear. This is thought to be due to the closure of microcracks and pore space in the rock with pressure (BIRCH 1961). Velocities determined at higher pressures are representative of the mineralogy and the orientation of the mineral grains. Velocities of the limestone sample range from 5.9 to 6.1 km s^{-1} at pressures >200 MPa. The density of the limestone was determined to be 2630 kg m^{-3} .

p (MPa)	v_{xy} (km s^{-1})	v_z (km s^{-1})
10	-	5.70
20	5.59	5.75
40	5.65	5.83
60	5.71	5.88
80	5.76	5.92
100	5.81	5.93
200	5.96	6.00
400	6.06	6.07
600	6.09	6.10

Tab. 4: Pressure (p), and P-wave velocity (v) of limestone sample NA-40B from Fossil Bay, Greenland. xy , parallel to foliation; z , normal to foliation.

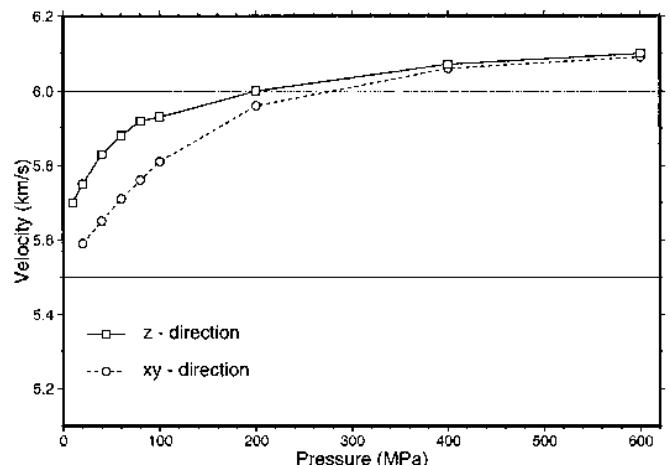


Fig. 9: P-wave velocities of a limestone sample (NA-40B) from Fossil Bay, Greenland, displayed as a function of pressure. Solid lines with squares show the results from the measurement normal to the foliation of the rock, dashed lines with circles correspond to the measurement parallel to the foliation.

DISCUSSION

Composition of upper layer

P-wave velocities of around 6.0 km s⁻¹ as observed in the upper layer of the three refraction seismic models in Kennedy Channel (Fig. 7) are normally interpreted as basement rocks (see typical crustal seismic velocities in HOLBROOK et al. 1992). However, when the Poisson's ratios of 0.28 to 0.32 are considered as well, there is no match to common crustal rock types. Based on the bedrock geology map (Fig. 8) of HARRISON (2006) carbonate deposits are likely to be the predominant lithology in Kennedy Channel. ANSELMETTI & EBERLI (2001) measured sonic velocities of carbonates from cores in the Great Bahama Bank and found that the *P*-wave velocities range between 1.9 and 6.4 km s⁻¹ and the *S*-wave velocities range between 1.0 and 3.5 km s⁻¹. The upper limit of this range covers the modeled *P*-wave (5.85–6.39 km s⁻¹) and *S*-wave velocities (3.05–3.35 km s⁻¹) observed on the three refraction seismic lines. In addition, the modeled *P*-wave velocities are very consistent with the measurements obtained from the limestone sample from Fossil Bay (5.9–6.1 km s⁻¹). This, together with the bedrock geology map of HARRISON (2006), strongly suggests that the upper layer in our velocity models is mainly composed of carbonate deposits.

Figure 8 shows the location of the zones where the lateral velocity transition occurs on the three refraction seismic lines. There is a reasonable correlation between this transition zone and the change of bedrock geology across Kennedy Channel from Upper Cambrian through Lower Silurian carbonate and evaporitic shelf deposits in the west to Silurian siliciclastic deposits and carbonate material in the east. The Silurian carbonate buildup around Hans Island cannot be resolved as a separate unit by the refraction seismic data. On line 1, the transition zone appears to be offset 2 km to the east compared to the change in bedrock geology. However, stations 1 and 2 are located off the shot line and therefore the exact position of the transition zone might be skewed. In summary, there is a good agreement between the bedrock geology and the physical properties (*P*-wave velocity and Poisson's ratio) in the upper sediment (carbonate) layer.

There is no information about the structure beneath the upper sediment layer, whether this is another sediment layer or crystalline basement. *P*-wave velocities underneath could well be lower than in the upper layer, given the high velocities within the carbonates. Higher velocities below the carbonates are not very likely because sediments generally have lower velocities and upper crustal rocks with a *P*-wave velocity >6.4 km s⁻¹ are not common unless they have a mafic composition. Basement velocities on refraction line 3 in southern Nares Strait (FUNCK et al. 2006) range from 5.95 to 6.15 km s⁻¹ for *P*-waves and from 3.44 to 3.55 km s⁻¹ for *S*-waves, which are consistent with a gneissic/granitic composition. Hence, if the underlying layer is composed of gneisses or granite, the velocity contrast at the base of the carbonates could be up to 0.4 km/s, sufficient to create the observed *P_bP* reflections. However, it cannot be excluded that there are siliciclastic sediments or carbonates with a lower velocity beneath the upper sediment layer in our velocity model.

Evidence for strike-slip movements?

One of the major objectives of the multidisciplinary research cruise was to look for evidence for or against strike-slip movement in Nares Strait. According to the plate reconstruction of SRIVASTAVA (1985), which is primarily based on magnetic seafloor anomalies, there is up to 150 km of northward movement of Greenland relative to North America. It is not easy to identify faults with the refraction seismic method, since the data do not provide a direct image of the subsurface structure. Instead, a velocity distribution (Fig. 7) is obtained by modeling. Some features in velocity models can possibly indicate a fault, such as a change in depth of layer boundaries or lateral velocity changes. However, these characteristics are often ambiguous.

In the case of the refraction seismic lines in Kennedy Channel, the lateral velocity change in the middle of the channel is not clear evidence for a strike-slip fault at that location as it could just as easily indicate a change of the depositional environment. If there were strike-slip motion in Kennedy Channel, a sharp variation in layer thickness could indicate the fault. This of course requires that the layer does not have a constant thickness. The depth to the base of the sediment layer on our three refraction seismic lines varies between 4.5 km in the south (line 1) to 3.5 km in the north (MCS line 8). It is reasonable to assume that this depth would vary across a transform fault with a possible offset of up to 150 km. The velocity models (Fig. 7) display constant depths along individual lines but Fig. 8 shows that the reflection midpoints sample only the eastern half of Kennedy Channel. The western half of the channel is not covered adequately due to the lack of shots between Carl Ritter Bay and Hans Island. However, even with the limited data set it can be concluded that the refraction data do not provide direct evidence for a strike-slip fault in the eastern part of Kennedy Channel (i.e. east of Hans Island).

This fits well with ideas of other authors who place the strike-slip motion in the coastal areas of Ellesmere Island, e.g., on Judge Daly Promontory (MAYR et al. in press, SAALMANN et al. 2005). JACKSON et al. (2006) map a steep fault just to the west of Hans Island (Fig. 8) based on reflection seismic and bathymetric data. They hypothesize that the near surface expression of this fault is the leading edge of the plate boundary between Greenland and North America.

CONCLUSIONS

The refraction seismic experiment in Kennedy Channel has provided key information needed for the interpretation of MCS data in the region. Because of its high velocity of c. 6 km s⁻¹, the upper sediment layer acted as acoustic basement in the MCS records (JACKSON et al. 2006), and the velocity and composition of the underlying material could not be determined. However, the *P*- and *S*-wave velocities obtained from the refraction seismic data (Fig. 7) indicate that the acoustic basement consists of carbonates. Significantly, the *P*-wave velocities of the upper sediment layer are similar to that of a limestone sample from Greenland (Fossil Bay) when measured at elevated pressures. This shows independently that there are high-velocity carbonates in the area.

Based on the seismic velocities, the carbonate layer has distinct properties in the western and eastern parts of Kennedy Channel. East of Hans Island, P -wave velocity ($v_p = 6.1$ - 6.2 km s⁻¹) and Poisson's ratio ($\sigma = 0.31$ - 0.32) are higher than to the west ($v_p = 5.8$ - 5.9 km s⁻¹; $\sigma = 0.28$ - 0.31). The boundary between these two units correlates well with variations shown on the geological map (HARRISON 2006), where carbonate mudrocks and fore-reef carbonates in the east are of Silurian age, and carbonates in the west are Late Cambrian through Early Silurian.

In eastern Kennedy Channel, the thickness of the carbonate layer could be determined by P_bP reflections. The base of the carbonates is at a depth of 4.5 km in the south (line 1) and 3.5 km in the north (line 8). The distribution of shots and receivers on the Ellesmerian side of the channel is insufficient to determine thickness there. We do not observe any major thickness variations of the carbonates within eastern Kennedy Channel. This is in agreement with the interpretation of the MCS data (JACKSON et al. 2006), which argues for a steep fault west of Hans Island to be the eastern boundary of the Wegener strike-slip Fault system that marks the plate boundary between North America and Greenland.

ACKNOWLEDGMENTS

We thank the officers, crew, helicopter pilots, technicians, and scientists onboard CCGS "Louis S. St-Laurent" for their support in carrying out the experiment. Alexander Grist provided the rock sample and Bob Iuliucci conducted the laboratory velocity measurements. We thank Randell Stephenson and Volkmar Damm for their helpful comments. The Nares Strait cruise was funded by the German Federal Agency of Geosciences and Natural Resources (BGR) and by the Geological Survey of Canada. Data analysis was covered by grants of the Danish National Research Foundation (Danmarks Grundforskningsfond). Geological Survey of Canada contribution 2004004.

- Anselmetti, F.S. & Eberli, G.P.* (2001): Sonic velocities in carbonates; a combined product of depositional lithology and diagenetic alterations.- In: R.N. Ginsburg (ed), Subsurface geology of a prograding carbonate platform margin, Great Bahama Bank; Results of the Bahamas Drilling Project.- Spec. Publ. Soc. Sediment. Geol. 70: 193-216.
- Birch, A.B.* (1960): The velocity of compressional waves in rocks to 10 kilobars, part 1.- J. Geophys. Res. 65: 1083-1102.
- Birch, A.B.* (1961): The velocity of compressional waves in rocks to 10 kilobars, part 2.- J. Geophys. Res. 66: 2199-2224.
- Dawes, P.R.* (2000): Kane Basin 1999: mapping, stratigraphic studies and economic assessment of Precambrian and Lower Palaeozoic provinces in north-western Greenland.- Geol. Greenland Surv. Bull. 186: 11-28.
- Dawes, P.R. & Kerr, J.W. (eds)* (1982a): Nares Strait and the drift of Greenland: A conflict in plate tectonics.- Meddel. om Grønland, Geosci. 8: 1-392.
- Dawes, P.R. & Kerr, J.W.* (1982b): The case against major displacement along Nares Strait.- Meddel. om Grønland, Geosci. 8: 369-386.
- Funck, T., Jackson, H.R., Dehler, S.A. & Reid, I.D.* (2006): A refraction seismic transect from Greenland to Ellesmere Island, Canada: The crustal structure in southern Nares Strait.- Polarforschung 74: 97-112.
- Harrison, J.C.* (in press): Bedrock geology Nares Strait, Map, scale 1:1.000.000.- Geol. Surv. Canada.
- Holbrook, W.S., Mooney, W.D. & Christensen, N.I.* (1992): The seismic velocity structure of the deep continental crust.- In: D.M. Fountain, R. Arculus & R. Kay (eds), Continental lower crust, Elsevier, Amsterdam, 1-43.
- Jackson, H.R., Hannon, T., Neben, S., Piepjohn, K. & Brent, T.* (2006): Seismic reflection profiles from Kane to Hall Basin, Nares Strait: Evidence for faulting.- Polarforschung 74: 21-39.
- Mayr, U., Tessensohn, F., Buggisch, W., de Freitas, T., Dewing, K., Estrada, S., von Gosen, W., Harrison, J.C., Henjes-Kunst, F., Lee, D., Lehnert, O., Melcher, F., Nowlan, G.S., Piepjohn, K., Saalman, K. & Sweet, A.R. (eds)*, (in press): The geology of northeast Ellesmere Island adjacent to Kane Basin and Kennedy Channel, Nunavut.- Geol. Surv. Canada Bull. 592.
- Saalman, K., Tessensohn, F., Piepjohn, K., von Gosen, W. & Mayr, U.* (2005): Structure of Palaeogene sediments in east Ellesmere Island: Constraints on Eureka tectonic evolution and implications for the Nares Strait problem.- Tectonophysics, 406: 81-113.
- Srivastava, S.P.* (1985): Evolution of the Eurasian Basin and its implications to the motion of Greenland along Nares Strait.- Tectonophysics 114: 29-53.
- Zelt, C.A. & Forsyth, D.A.* (1994): Modeling wide-angle seismic data for crustal structure: Southeastern Grenville Province.- J. Geophys. Res. 99: 11687-11704.
- Zelt, C.A., & Smith, R.B.* (1992): Seismic traveltimes inversion for 2-D crustal velocity structure.- Geophys. J. Internat. 108: 16-34.